Journal of Solid State Chemistry **151,** 96–101 (2000)
doi:10.1006/jssc.2000.8627, available online at http://www.idealibrary.com on IDEAL®

Analysis of the Spin Exchange Interactions in the Extended Magnetic Solids K_2NiF_4, K_2CuF_4, La_2CuO_4, Nd_2CuO_4, $KNiF_3$, and $KCuF_3$

H.-J. Koo and M.-H. Whangbo[1]

Department of Chemistry, North Carolina State University, Raleigh, North Carolina 27695-8204

Received November 8, 1999; in revised form December 22, 1999; accepted January 10, 2000

The spin exchange parameters J of the extended magnetic solids K_2NiF_4, K_2CuF_4, La_2CuO_4, Nd_2CuO_4, $KNiF_3$, and $KCuF_3$ were analyzed by examining the structures of their spin monomers and calculating the energy differences Δe in the spin levels of their spin dimers. The trends in the observed J parameters are well explained in terms of the Δe values obtained from extended Hückel molecular orbital calculations. The Δe value of a spin dimer is related only to the antiferromagnetic component of its J, but the spin dimer analysis based on Δe allows one to correlate the nature of the magnetic interaction with the structure of the spin dimer. © 2000 Academic Press

Key Words: **spin exchange interactions; magnetically ordered materials; extended Hückel molecular orbital calculations.**

1. INTRODUCTION

The magnetic interactions between adjacent spins in an extended magnetic solid are generally studied by analyzing the temperature dependence of its magnetic susceptibility (1). The latter can be calculated in terms of a spin Hamiltonian by treating the nearest-neighbor spin exchange parameters J as adjustable numerical parameters. Thus by fitting the observed magnetic susceptibility versus temperature curve with the calculated one, one can derive the J values and hence gain insight into the magnetic interactions between adjacent spins. To relate the trends in the J values to the crystal structure of a magnetic system, it is necessary to perform appropriate electronic structure calculations for "spin monomers" (i.e., structural units containing an unpaired spin) and "spin dimers" (i.e., structural units containing two adjacent unpaired spins) of the system (2–10). The J parameter of a spin dimer is generally related to the energy difference ΔE between the triplet and singlet states of the dimer as $J = \Delta E = {}^1E - {}^3E$, where ${}^1E$ and ${}^3E$ are the total energies of the singlet and triplet states, respectively. Thus the interaction between adjacent spins is ferromagnetic if the triplet state is more stable than the singlet state, and is antiferromagnetic otherwise. In general, J can be written as $J = J_F + J_{AF}$, where the ferromagnetic term J_F favors the triplet state (i.e., $J_F > 0$), and the antiferromagnetic term J_{AF} favors the singlet state (i.e., $J_{AF} < 0$) (1, 11, 12).

Qualitative trends in the J parameters of a magnetic system can be probed in terms of one-electron orbital picture (1–4, 12). For the interaction between two equivalent spins, suppose that Δe is the energy gap between the two singly occupied energy levels of a spin dimer (Fig. 1). Then J_{AF} is related to Δe as $J_{AF} \propto -(\Delta e)^2$ (12). Thus to understand the qualitative trends in the J parameters of a magnetic system in terms of its crystal structure, one needs to examine the variations of the corresponding Δe values. When Δe is large, it is likely that the corresponding J is dominated by J_{AF}, and the magnetic interaction is antiferromagnetic. When Δe is small, it is likely that the corresponding J is dominated by J_F, and the magnetic interaction is ferromagnetic. The spin dimer analysis based on the Δe values calculated from extended Hückel molecular orbital (EHMO) calculations (13) has been successfully used to explain the antiferromagnetic properties of the vanadium oxides $[H_2N(CH_2)_4NH_2]V_4O_9$, CaV_4O_9 and $Cs_2V_4O_9$ (2), α'-NaV_2O_5, CaV_2O_5 and MgV_2O_5 (4), MV_3O_7 (M = Cd, Ca, Sr) and β-Ba_2VO_4 (14), as well as the K_4CdCl_6-type oxides $A_3M'MO_6$ (M = Rh, Ir; A = Ca, Sr; M' = alkaline earth, Zn, Cd, Na) (3).

The magnetic properties of three-dimensional perovskites $KNiF_3$ and $KCuF_3$, the layered perovskites K_2NiF_4, K_2CuF_4, and La_2CuO_4, and the layered oxide Nd_2CuO_4 have been extensively studied both theoretically (5–10) and experimentally (15–24). The J values of K_2NiF_4, K_2CuF_4, La_2CuO_4, $KNiF_3$, and $KCuF_3$ were examined by calculating their spin dimer ΔE values in a number of first principles electronic structure studies (5–8, 10), and so were the J values of La_2CuO_4 and Nd_2CuO_4 in a semiempirical electronic structure study (9). As summarized in Table 1 and Fig. 2a, this total energy approach leads to a nearly quantitative description of J but does not provide a qualitative conceptual framework in which to think about magnetic

[1] To whom correspondence should be addressed.

0022-4596/00 $35.00

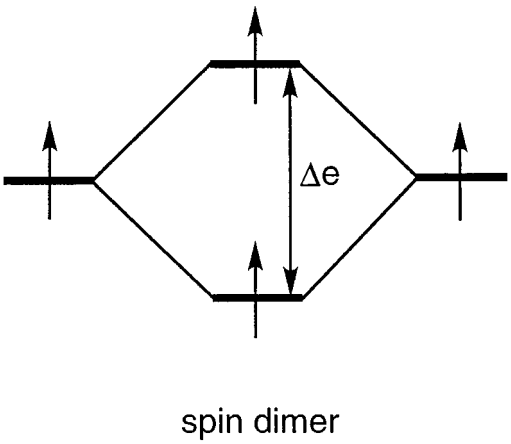

FIG. 1. Interaction between adjacent spin orbitals in a spin dimer leading to the one-electron energy gap Δe.

interactions in terms of the crystal structure. Several important questions concerning the magnetic solids K_2NiF_4, K_2CuF_4, La_2CuO_4, Nd_2CuO_4, $KNiF_3$, and $KCuF_3$ are (a) why the *ab*-plane magnetic interactions of $KCuF_3$ and K_2CuF_4 are ferromagnetic while the *c*-direction magnetic interactions of $KCuF_3$ are antiferromagnetic, (b) why $KNiF_3$ and K_2NiF_4 are antiferromagnetic to a similar extent but are much more weakly antiferromagnetic than $KCuF_3$, and (c) why the J values of K_2NiF_4, K_2CuF_4, La_2CuO_4, Nd_2CuO_4, $KNiF_3$, and $KCuF_3$ exhibit the ordering shown in Fig. 2a. In the present work, we probe these questions by analyzing the crystal structures of K_2NiF_4, K_2CuF_4, La_2CuO_4, Nd_2CuO_4, $KNiF_3$, and $KCuF_3$ and calculating the spin dimer Δe values on the basis of EHMO calculations (25), for which the valence atomic orbitals of Ni, Cu, O, and F were represented by double-ζ Slater-type orbitals (25, 26). The atomic parameters of Ni, Cu, O, and F employed in our calculations are summarized in Table 2.

TABLE 1
Comparison of the Experimental J Parameters with Calculated ΔE and Δe Values

Compound	J (meV)	Calculated ΔE (meV)	Calculated Δe (meV)
K_2CuF_4	1.5,[a] 1.9[b]	1.21[k]	12
$KCuF_3$	−33,[c] −34,[d] −35[e]	−31.3[k]	161
	0.34[e]	0.56[l]	20
K_2NiF_4	−8.2,[f] −9.5[f]	−8.10[k]	197
$KNiF_3$	−7.7[g]	−7.41[k]	186
Nd_2CuO_4	−108[h]	−117[m]	422
La_2CuO_4	−128,[h,i] −134[j]	−144.7,[k] −134[m]	448

[a] Ref. 20. [b] Ref. 21. [c] Ref. 17. [d] Ref. 18. [e] Ref. 19. [f] Ref. 16. [g] Ref. 15. [h] Ref. 23. [i] Ref. 22. [j] Ref. 24. [k] Ref. 8. [l] Ref. 5. [m] Ref. 9.

2. STRUCTURES OF SPIN MONOMERS AND DIMERS

$KNiF_3$ consists of corner-sharing regular NiF_6 octahedra (27), while K_2NiF_4 (28), K_2CuF_4 (29), La_2CuO_4 (30), and $KCuF_3$ (31) have corner-sharing distorted MX_6 octahedra (M = Ni, Cu, X = F; M = Cu, X = O). Nd_2CuO_4 (32, 33) contains corner-sharing CuO_4 squares. The oxidation state of the transition metal atoms is +2 in these compounds, and so the spin monomers are the $(CuF_6)^{4-}$ octahedral clusters in $KCuF_3$ and K_2CuF_4, the $(NiF_6)^{4-}$ octahedral clusters in $KNiF_3$ and K_2NiF_4, the $(CuO_6)^{10-}$ octahedral clusters in La_2CuO_4, and the $(CuO_4)^{6-}$ square planar clusters in Nd_2CuO_4. For convenience, the M–X bonds along the *c*-direction and in the *ab*-plane may be referred to as

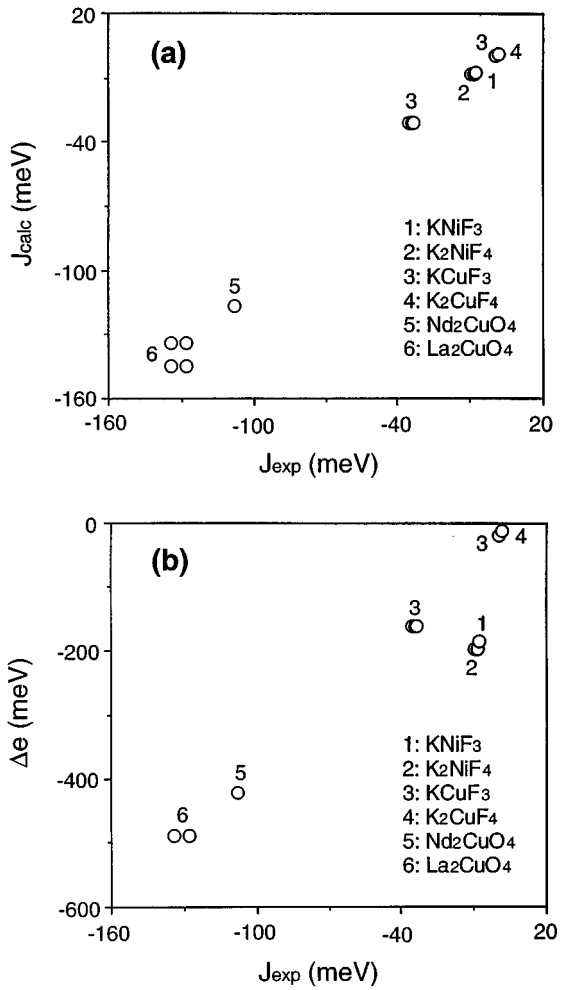

FIG. 2. (a) Plot of the experimental J parameters versus the calculated ΔE values. (b) Plot of the experimental J parameters versus the calculated Δe values. The sources of the J and ΔE data used in these plots are specified in Table 1.

TABLE 2

Exponents ζ_i and Valence Shell Ionization Potentials H_{ii} of Slater-Type Orbitals χ_i Used for Extended Hückel Tight-Binding Calculation[a]

Atom	χ_i	H_{ii} (eV)	ζ_i	c_1[b]	ζ_i'	c_2[b]
Ni	4*s*	− 9.17	2.077	1.0		
Ni	4*p*	− 5.15	1.470	1.0		
Ni	3*d*	− 13.5	6.076	0.4212	2.874	0.7066
Cu	4*s*	− 6.59	2.151	1.0		
Cu	4*p*	− 3.33	1.370	1.0		
Cu	3*d*	− 15.2	7.025	0.4473	3.004	0.6968
O	2*s*	− 32.3	2.688	0.7076	1.675	0.3745
O	2*p*	− 14.8	3.694	0.3322	1.659	0.7448
F	2*s*	− 40.0	3.136	0.6737	1.945	0.4144
F	2*p*	− 18.1	4.184	0.3546	1.851	0.7299

[a] H_{ii}'s are the diagonal matrix elements $\langle\chi_i|H^{\text{eff}}|\chi_i\rangle$, where H^{eff} is the effective Hamiltonian. In our calculations of the off-diagonal matrix elements $H^{\text{eff}} = \langle\chi_i|H^{\text{eff}}|\chi_j\rangle$, the weighted formula was used. See: J. Ammeter, H.-B. Bürgi, J. Thibeault, and R. Hoffmann, *J. Am. Chem. Soc.* **100,** 3686 (1978).

[b] Contraction coefficients used in the double-ζ Slater-type orbital.

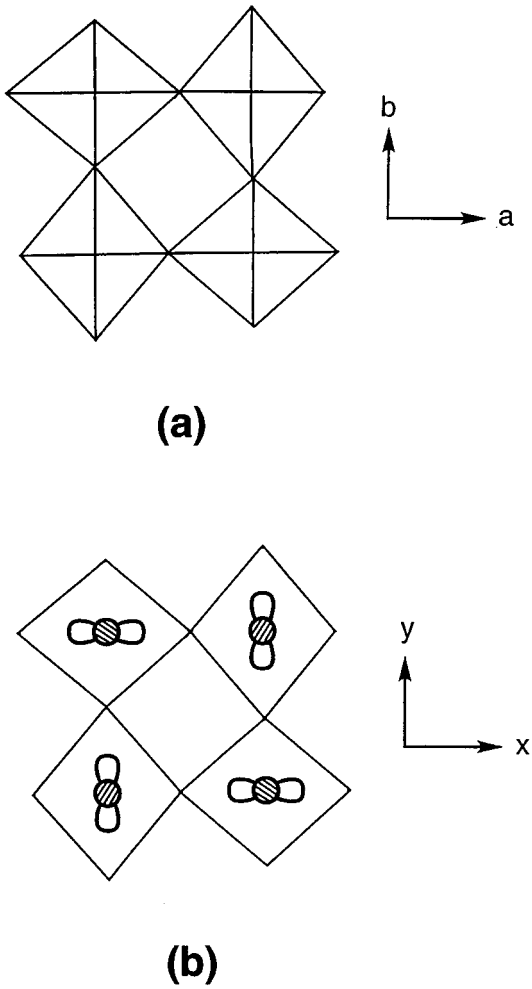

FIG. 3. (a) Schematic projection view of the $Cu(F_{eq})_2$ sheets present in $KCuF_3$ and K_2CuF_4. Each square represents a $Cu(F_{eq})_4$ square. (b) Schematic projection view of the spin orbitals z^2–x^2 and z^2–y^2 present at the Cu sites of each $Cu(F_{eq})_2$ sheet.

M–X_{ax} and M–X_{eq}, respectively. Table 3 summarizes the lengths of these bonds found for the various spin monomers. From the viewpoint of a regular octahedral structure, the $(CuF_6)^{4-}$ and $(CuO_6)^{10-}$ clusters show a stronger distortion than do the $(NiF_6)^{4-}$ clusters. This is easily explained in terms of Jahn–Teller instability (34, 35). If the spin monomers $(CuF_6)^{4-}$ and $(CuO_6)^{10-}$ had a regular octahedral structure, their doubly degenerate e_g-block levels would have three electrons. Such spin monomers should undergo a Jahn–Teller distortion so that the distorted spin monomer accommodates an unpaired spin in the highest-lying *d*-block level (see below). If the spin monomer $(NiF_6)^{4-}$ had a regular octahedral structure, its two e_g-block levels each would have an unpaired spin. Thus the spin monomer $(NiF_6)^{4-}$ has no Jahn–Teller instability as long as it keeps this high-spin configuration. The weak distortion of $(NiF_6)^{4-}$ found in layered perovskite K_2NiF_4 is not caused by a Jahn–Teller distortion, but rather by the anisotropic environment of the layered structure.

TABLE 3

Spin Orbitals and M–X Bond Lengths of the Spin Monomers

Compound	M–X_{ax}	M–X_{eq}	Spin orbital
$KNiF_3$[a]	2.006 (×2)	2.006 (×4)	x^2–y^2, z^2
K_2NiF_4[b]	1.982 (×2)	1.997 (×4)	x^2–y^2, z^2
$KCuF_3$[c]	1.962 (×2)	1.889 (×2)	z^2–x^2 or z^2–y^2
		2.253 (×2)	
K_2CuF_4[d]	1.939 (×2)	1.909 (×2)	z^2–x^2 or z^2–y^2
		2.238 (×2)	
La_2CuO_4[e]	2.465 (×2)	1.907 (×4)	x^2–y^2
Nd_2CuO_4[f]		1.973 (×4)	x^2–y^2

[a] Ref. 27. [b] Ref. 28. [c] Ref. 31. [d] Ref. 29. [e] Ref. 30. [f] Ref. 32.

According to Table 3, the $M(X_{eq})_2$ sheets (parallel to the *ab*-plane) of K_2NiF_4, K_2CuF_4, La_2CuO_4, Nd_2CuO_4, $KNiF_3$, and $KCuF_3$ are divided into two classes. Fig. 3a depicts the $Cu(F_{eq})_2$ sheets present in $KCuF_3$ and K_2CuF_4, and Fig. 4a those in $KNiF_3$, K_2NiF_4, Nd_2CuO_4, and La_2CuO_4. In each $(CuF_6)^{4-}$ cluster of $KCuF_3$ and K_2CuF_4, the Cu–F_{ax} bond is shorter than the longer Cu–F_{eq} bond. Thus the e_g-block levels of $(CuF_6)^{4-}$ become hybridized such that the highest-lying *d*-block level becomes either the z^2–x^2 or the z^2–y^2 orbital (34, 35), and these spin orbitals alternate along the *a*- and *b*-directions in the $Cu(O_{eq})_2$ sheet (Fig. 3b). Each $(NiF_6)^{4-}$ cluster of $KNiF_3$ and K_2NiF_4 has two unpaired spins, which are accommodated in the x^2–y^2 and z^2 orbitals (Figs. 4b, 4c). In the

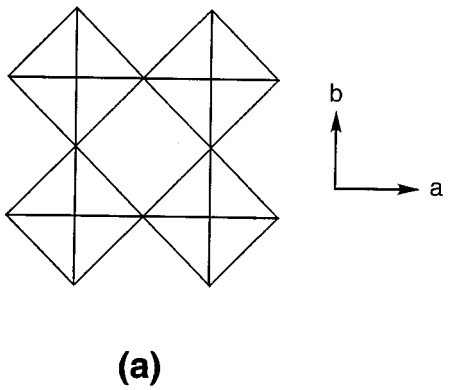

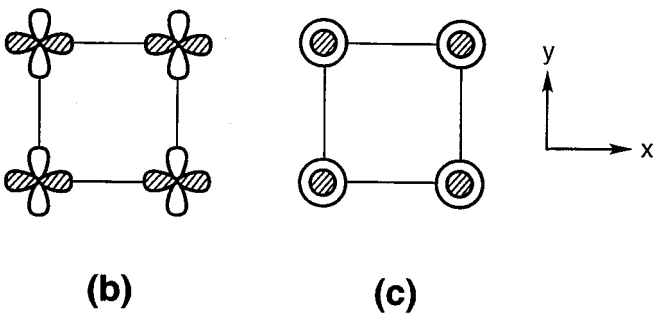

FIG. 4. (a) Schematic projection view of the $M(X_{eq})_2$ (M = Ni, X = F; M = Cu, X = O) sheets present in $KNiF_3$, K_2NiF_4, Nd_2CuO_4, and La_2CuO_4. Each square represents an $M(X_{eq})_4$ square. Schematic projection views of the x^2–y^2 and z^2 spin orbitals present at the M sites of each $M(X_{eq})_2$ sheet are shown in (b) and (c), respectively. The $Cu(O_{eq})_2$ sheet of La_2CuO_4 is not completely flat but has a washboard-type corrugation, so that each Cu–O_{eq}–Cu linkage is bent with $\angle$Cu–O_{eq}–Cu = 174.45.

$(CuO_6)^{10-}$ cluster of La_2CuO_4 and the $(CuO_4)^{6-}$ cluster of Nd_2CuO_4, an unpaired spin resides in the x^2–y^2 orbital (Fig. 4b). Adjacent spin monomers share a corner to form spin dimers so that spin dimers are the $(Cu_2F_{11})^{7-}$ clusters in $KCuF_3$ and K_2CuF_4, the $(Ni_2F_{11})^{7-}$ clusters in $KNiF_3$ and K_2NiF_4, the $(Cu_2O_{11})^{18-}$ clusters in La_2CuO_4, and the $(Cu_2O_7)^{10-}$ clusters in Nd_2CuO_4.

3. RESULTS AND DISCUSSION

In a spin dimer the spin-containing d-block orbitals interact via the M–X–M bridge. As a result, only the interaction involving the d-orbitals with lobes pointed along the shared corner atom leads to a large Δe value (36), as depicted in Figs. 5a and 5b. Consequently, the interaction between the x^2–y^2 orbitals along the a- and b-directions (Fig. 6a), that between the z^2–x^2 (or z^2–y^2) orbitals along the c-direction, and that between the z^2 orbitals along the c-direction (Fig. 6b) give rise to a large Δe value and hence are likely to be antiferromagnetic. The interaction between other combinations of adjacent spin orbitals (Fig. 6c–6e) leads to a small Δe value and is likely to be ferromagnetic. The Δe values calculated for the various spin dimers are listed in Table 1.

The Δe value of K_2CuF_4 calculated for the a- and b-directions is small (12 meV), which should be related to the observed ferromagnetism in K_2CuF_4. For $KCuF_3$ the Δe value for the a- and b-directions is small (20 meV), but that for the c-direction is large (161 meV). Thus it is understandable why $KCuF_3$ is ferromagnetic along the a- and b-directions and is antiferromagnetic along the c-direction. Ultimately, the Jahn–Teller distortion in each spin monomer $(CuF_6)^{4-}$ is responsible for why the magnetic interactions of K_2CuF_4 and $KCuF_3$ are ferromagnetic in the

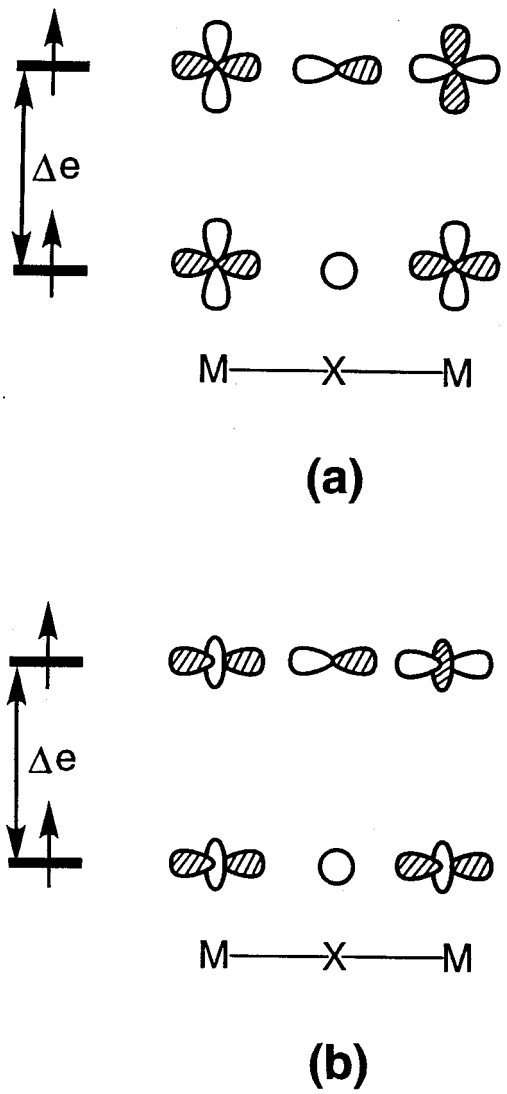

FIG. 5. Two types of interactions between the d-orbitals in a spin dimer across the shared corner that lead to a large Δe value. The spin orbitals in (a) may represent the x^2–y^2, z^2–x^2, or z^2–y^2 orbitals, while those in (b) represent the z^2 orbitals.

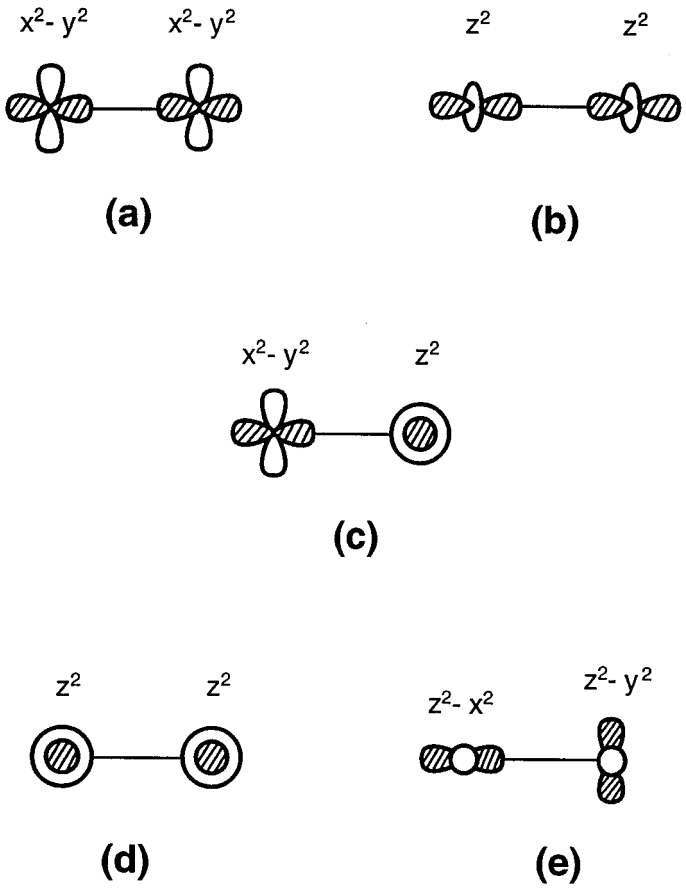

FIG. 6. Various combinations of adjacent spin orbitals. The combinations in (a) and (b) lead to a large Δe value, while those in (c), (d), and (e) lead to a small Δe value.

ab-plane and why those of $KCuF_3$ are antiferromagnetic along the *c*-direction. The distortion makes the unpaired spins reside in the z^2–x^2 and z^2–y^2 orbitals. The interactions between adjacent z^2–x^2 and z^2–y^2 orbitals in the *ab*-plane are weak, but those between z^2–x^2 (or z^2–y^2) orbitals along the *c*-direction are strong.

The Δe values of $KNiF_3$ are large (186 meV) for the interactions between the x^2–y^2 orbitals along the *a*- and *b*-directions and between the z^2 orbitals along the *c*-direction. The Δe values of K_2NiF_4 are large (197 meV) for the interactions between the x^2–y^2 orbitals along the *a*- and *b*-directions. These Δe values are larger than that of $KCuF_3$ along the *c*-direction (i.e., 161 meV). Nevertheless, the *J* values of $KNiF_3$ and K_2NiF_4 (-7.7 and -9.5 meV, respectively) are considerably smaller in magnitude than that of $KCuF_3$ (i.e., -34 meV). Each Ni^{2+} ion of $KNiF_3$ and K_2NiF_4 has two unpaired spins in the x^2–y^2 and z^2 orbitals. Therefore, in a given spin dimer $(Ni_2F_{11})^{7-}$, one antiferromagnetic interaction is likely to be counterbalanced by three ferromagnetic interactions. For example, for a spin dimer contained in the *ab*-plane, the interaction between the x^2–y^2 orbitals is antiferromagnetic, while those between the z^2 orbitals, between the x^2–y^2 and z^2 orbitals, and between the z^2 and x^2–y^2 orbitals are ferromagnetic. This explains why the antiferromagnetic interaction is stronger in $KCuF_3$ than in $KNiF_3$ and K_2NiF_4, although $KCuF_3$ has a smaller Δe value.

Figure 2b plots the experimental *J* values against the calculated Δe values. The Cu-containing compounds, which have one unpaired spin per Cu^{2+}, show that the magnitude of *J* increases continuously (almost linearly) with increasing Δe. The Ni-containing compounds $KNiF_3$ and K_2NiF_4, which have two unpaired spins per Ni^{2+}, do not follow this relationship. This is not surprising because the experimental *J* has both ferromagnetic and antiferromagnetic contributions whereas the Δe value is related only to the antiferromagnetic part of *J*. As discussed above, the overall antiferromagnetic interaction in the spin dimer $(Ni_2F_{11})^{7-}$ is reduced in magnitude due to the ferromagnetic interactions associated with two spin orbitals on each Ni^{2+} site. The Δe value of Nd_2CuO_4 is substantially larger than that of $KCuF_3$ (i.e., 448 vs 161 meV), although the *M*–*X*–*M* bridge of the spin dimer has a longer *M*–*X* bond in Nd_2CuO_4 than in $KCuF_3$ (i.e., 1.973 vs 1.962 Å). In terms of orbital interactions (37), this reflects the fact that the O 2*p* orbital is less contracted than the F 2*p* orbital, and the O 2*p* level is closer in energy to the Cu 3*d* orbital than is the F 2*p* level. The Δe value of La_2CuO_4 is larger than that of Nd_2CuO_4 (i.e., 448 vs 422 meV), in agreement with the observation that the Cu–O_{eq}–Cu bridge of the spin dimer has a shorter Cu–O_{eq} bond in La_2CuO_4 than in Nd_2CuO_4 (i.e., 1.907 vs 1.973 Å). However, the difference in the Δe values of these two oxides is small compared with the large difference in their Cu–O_{eq} bond lengths. This is explained by the fact that the Cu–O_{eq}–Cu linkage is linear in Nd_2CuO_4, but is bent in La_2CuO_4 ($\angle$Cu–O_{eq}–Cu = 174.45°). The bending of the Cu–O_{eq}–Cu linkage reduces the overlap between the Cu 3*d* and O 2*p* orbitals in the Cu–O_{eq} bond, thereby decreasing the associated Δe value.

4. CONCLUDING REMARKS

The interactions between nearest-neighbor spins in an extended magnetic solid are described by spin exchange parameters *J*. In terms of electronic structure calculations, the *J* value for the interaction between adjacent spins is generally related to the singlet–triplet energy difference ΔE of the spin dimer containing the two spins. This total energy approach can reproduce experimental *J* values almost quantitatively (5–10). The one-electron orbital energy difference Δe calculated for a spin dimer is related only to the antiferromagnetic component J_{AF} of its *J*. Nevertheless, the spin dimer analysis based on Δe makes it possible to correlate the magnetic interaction with the structure of the spin

dimer. The trends in the J values of K_2NiF_4, K_2CuF_4, La_2CuO_4, Nd_2CuO_4, $KNiF_3$, and $KCuF_3$ are well explained in terms of the Δe values calculated for their spin dimers. The variation of Δe can be easily understood in terms of simple bonding concepts such as bond length, overlap, and symmetry. Therefore, the spin dimer analysis based on Δe provides a qualitative conceptual framework in which to think about magnetic interactions.

ACKNOWLEDGMENTS

This work was supported by the Office of Basic Energy Sciences, Division of Materials Sciences, U.S. Department of Energy, under Grant DE-FG05-86ER45259.

REFERENCES

1. For a recent review, see: O. Kahn, "Molecular Magnetism." VCH Publishers, Weinheim, 1993.
2. Y. Zhang, C. J. Warren, R. C. Haushalter, A. Clearfield, D.-K. Seo, and M.-H. Whangbo, *Chem. Mater.* **10,** 1059 (1998).
3. K.-S. Lee, H.-J. Koo, and M.-H. Whangbo, *Inorg. Chem.* **38,** 2199 (1999).
4. H.-J. Koo and M.-H. Whangbo, *Solid State Commun.* **111,** 353 (1999).
5. I. de P. R. Moreira and F. Illas, *Phys. Rev. B* **60,** 5179 (1999).
6. J. Casanovas and F. Illas, *J. Chem. Phys.* **100,** 8257 (1994).
7. J. Casanovas, J. Rubio, and F. Illas, *Phys. Rev. B* **53,** 945 (1996).
8. I. de P. R. Moreiro, F. Illas, C. J. Calzado, J. F. Sanz, J.-P. Malrieu, N. B. Amor, and D. Maynau, *Phys. Rev. B* **59,** 6593 (1999).
9. Y. J. Wang, M. D. Newton, and J. W. Davenport, *Phys. Rev. B* **46,** 11935 (1992).
10. A. B. van Oosten, R. Broer, and W. C. Nieuwpoort, *Chem. Phys. Lett.* **257,** 207 (1996).
11. P. W. Anderson, *in* "Magnetism" (G. T. Rado and H. Suhl, eds.), vol. 1, p. 25. Academic Press, NewYork, 1963.
12. P. J. Hay, J. C. Thibeault, and R. Hoffmann, *J. Am. Chem. Soc.* **97,** 4884 (1975).
13. R. Hoffmann, *J. Chem. Phys.* **39,** 1397 (1963).
14. M.-H. Whangbo and H.-J. Koo, *Solid State Commun.*, in press.
15. M. E. Lines, *Phys. Rev.* **164,** 736 (1967).
16. L. J. de Jongh and R. Miedema, *Adv. Phys.* **23,** 1 (1974).
17. S. Katoda, I. Yamada, S. Yoneyama, and K. Hirakawa, *J. Phys. Soc. Jpn.* **23,** 751 (1967).
18. M. T. Hutchings, E. J. Samuelson, G. Shirane, and K. Hirakawa, *Phys. Rev.* **188,** 919 (1969).
19. S. K. Satija, J. D. Axe, G. Shirane, H. Yonezawa, and K. Hirakawa, *Phys. Rev. B* **21,** 2001 (1980).
20. I. Yamada, *J. Phys. Soc. Jpn.* **33,** 979 (1972).
21. K. Hirakawa and H. Ikeda, *J. Phys. Soc. Jpn.* **35,** 1328 (1973).
22. R. R. P. Singh, P. A. Fleury, K. B. Lyons, and P. E. Sulewski, *Phys. Rev. Lett.* **62,** 2736 (1989).
23. P. E. Sulewski, P. A. Fleury, K. B. Lyons, S.-B. Cheong, and Z. Fisk, *Phys. Rev. B* **41,** 225 (1990).
24. G. Aeppli, S. M. Hayden, H. A. Mook, Z. Fisk, S.-W. Cheong, D. Rytz, J. P. Remeika, G. P. Espinosa, and A. S. Cooper, *Phys. Rev. Lett.* **62,** 2052 (1989).
25. Our calculations were carried out by employing the CAESAR program package: J. Ren, W. Liang and M.-H. Whangbo, "Crystal and Electronic Structure Analysis Using CAESAR," 1998. This book can be downloaded free of charge from the Web site http://www.PrimeC.com/.
26. E. Clementi and C. Roetti, *At. Data Nuclear Data Tables* **14,** 177 (1974).
27. K. Knox, *Acta Crystallogr.* **14,** 583 (1961).
28. D. Balz, *Naturwissenschaften* **40,** 241 (1953).
29. E. Herdtweck and D. Babel, *Z. Anorg. Allg. Chem.* **474,** 113 (1981).
30. B. Grande, Hk. Müller-Buschbaum, and M. Schweitzer, *Z. Anorg. Allg. Chem.* **428,** 120 (1977).
31. R. H. Buttner, E. N. Maslen, and N. Spadaccini, *Acta Crystallogr. B* **46,** 131 (1990).
32. Hk. Müller-Buschbaum and W. Wollschläger, *Z. Anorg. Allg. Chem.* **414,** 76 (1975).
33. H. Wilhelm, C. Cros, E. Reny, G. Demazeau, and M. Hanfland, *J. Mater. Chem.* **8,** 2729 (1998).
34. D. I. Khomski and K. I. Kugel, *Solid State Commun.* **13,** 763 (1973).
35. Y. Ito and J. Akimitsu, *J. Phys. Soc. Jpn.* **40,** 1333 (1976).
36. E. Canadell and M.-H. Whangbo, *Chem. Rev.* **91,** 965 (1991).
37. T. A. Albright, J. K. Burdett, and M.-H. Whangbo, "Orbital Interactions in Chemistry," Chap. 2. Wiley, New York, 1985.